THE EFFECTS OF AN IMPOSED MAGNETIC FIELD ON NATURAL CONVECTION IN A TILTED CAVITY WITH PARTIALLY ACTIVE VERTICAL WALLS: NUMERICAL APPROACH

G.A. Sheikhzadeh*, M.R. Babaei and V. Rahmany

Department of Mechanical Engineering, University of Kashan
Post Code 87317-51167, Kashan, Iran
sheikhz@kashanu.ac.ir - mrb_6079@yahoo.com - rahmanivahid@yahoo.com

M.A. Mehrabian

Department of Mechanical Engineering, Shahid Bahonar University of Kerman
P.O. Box 76169-133, Kerman, Iran
ma_mehrabian@yahoo.com

*Corresponding Author

(Received: January 24, 2008 – Accepted in Revised Form: July 2, 2009)

Abstract The effect of imposed magnetic field on natural convection in a tilted cavity with partially active walls was investigated numerically. The active part of the right side wall was at a higher temperature than the active part of the left side wall and were moving on vertical walls relative to each other. The top, the bottom and the remaining parts of the side walls were insulated. The magnetic field was perpendicular to the side walls. The SIMPLER algorithm was used to indicate the pressure gradient in the momentum equations. Flow field and heat transfer were predicted for fluid with Pr = 0.71 and a wide range of the governing parameters such as Rayleigh number between 10^4 and 10^6, Hartmann number between 0 and 100, aspect ratio between 0.5 and 2 and inclination angle between 0° and 90°. The average Nusselt number decreased with an increase of Hartmann number and increased with an increase of Rayleigh number. The maximum heat transfer rate was occurred for the middle–middle thermally active locations while heat transfer was poor for the bottom-top thermally active locations.

Keywords Magnetic Field, Natural Convection, Partially Active Walls, Cavity

چکیده تأثیر میدان مغناطیسی اعمالی بر جریان جابجایی آزاد در یک محفظهٔ مایل با دیواره‌های به طور جزئی فعال به طور عددی مطالعه شده است. بخش فعال دیوار سمت راست در دمای بالاتری نسبت به بخش فعال دیوار سمت چپ قرار دارد و نسبت به یکدیگر بر روی دیواره‌های عمودی حرکت می‌کنند. دیواره‌های بالا، پایین و بخش‌های دیگر دیواره‌های جانبی عایق می‌باشند. میدان مغناطیسی عمود بر دیواره‌های جانبی می‌باشد. الگوریتم سیمپلر به منظور ارزیابی گرادیان فشار در معادلات مومنتوم مورد استفاده قرار گرفته است. میدان جریان و انتقال حرارت برای سیالی با Pr =۰/۷۱ و محدوده گسترده‌ای از پارامترهای حاکم نظیر عدد رایلی بین $۱۰^٤$ تا $۱۰^٦$، عدد هارتمن بین ۰ و ۱۰۰، نسبت ابعاد بین ۰/۵ و ۲ و زاویهٔ انحراف بین ۰ و ۹۰ درجه مورد بررسی قرار گرفته است. عدد ناسلت متوسط با افزایش عدد هارتمن کاهش و با افزایش عدد رایلی افزایش می‌یابد. بیشترین نرخ انتقال حرارت مربوط به قرارگیری بخش فعال حرارتی در موقعیت مرکز–مرکز می‌باشد و این در حالی است که انتقال حرارت برای قرارگیری بخش فعال حرارتی در موقعیت پایین–بالا ضعیف می‌باشد.

1. INTRODUCTION

Magneto-convection occurs under many circumstances and received a great deal of attention as it finds applications in geophysics, astrophysics, aerodynamics, engineering and industries [1]. Magneto-convection in cavities particularly has applications in solar technologies, safety aspects of gas cooled reactors, crystal growth in liquids, material manufacturing technology and haemodialysis. There are situations where heat is being generated during certain operations and

may be detrimental to the equipment. The undesirable amount of heat has to be removed as far as possible. For instance gas turbine blades, walls of an I. C. engine combustion chamber, outer surface of a space vehicle, all depend on their durability on rapid heat removal from their surfaces. Natural convection in a rectangular cavity with differentially heated side walls and insulated horizontal surfaces has been the subject of great interest.

When the fluid is electrically conducting and exposed to a magnetic field, the Lorentz force is also active and interacts with the buoyancy force in governing the flow and temperature fields. Employment of an external magnetic field has increasing applications in material manufacturing industry as a control mechanism since the Lorentz force suppresses the convection currents by reducing the velocities. Study and thorough understanding of the momentum and heat transfer in such a process is important for the better control and quality of the manufactured products. The study of Oreper, et al [2] shows that the magnetic field suppresses the natural-convection currents and the magnetic field strength is one of the most important factors for crystal formation. Ozoe, et al [3] numerically investigated the natural convection of a low Prandtl number fluid in the presence of a magnetic field and obtained correlations for the Nusselt number in terms of Rayleigh, Prandtl and Hartmann numbers. Garandet, et al [4] proposed an analytical solution to the governing equations of magnetohydrodynamics to be used to model the effect of a transverse magnetic field on natural convection in a two-dimensional cavity. Rudraiah, et al [5] numerically investigated the effect of a transverse magnetic field on natural-convection flow inside a rectangular enclosure with isothermal vertical walls and adiabatic horizontal walls and found out that a circulating flow is formed with a relatively weak magnetic field and that the convection is suppressed and the rate of convective heat transfer is decreased when the magnetic field strength increases. Alchaar, et al [6] numerically investigated the natural convection in a shallow cavity heated from below in the presence of an inclined magnetic field and showed that the convection modes inside the cavity strongly depend on both the strength and orientation of the magnetic field and that horizontally applied magnetic field is the most effective in suppressing the convection. Al-Najem, et al [7] used the power law control volume approach to determine the flow and temperature fields under a transverse magnetic field in a tilted square enclosure with isothermal vertical walls and adiabatic horizontal walls at Prandtl number of 0.71 and showed that the suppression effect of the magnetic field on convection and heat transfer is more significant for low inclination angles and high Grashof numbers. Kandaswamy, et al [8] numerically investigated flow and temperature fields in a square cavity with partially active vertical walls for Prandtl number of 0.71. The active part of the left side wall is at a higher temperature than the active part of the right side wall. The top, bottom and the inactive parts of the side walls are thermally inactive. They found that heat transfer rate is maximum for the middle-middle thermally active locations while it is poor for the top-bottom thermally active locations. Babaei [9] with numerical procedure investigated the effect of imposing a constant magnetic field on a natural convection flow and temperature field in a laminar steady state flow through an enclosure containing molten gallium with prandtl number equal to 0.02. Also the enclosure has lateral walls with boundary conditions of constant temperature and constant heat flux. Moreover, in order to achieve to comprehensive results, besides the studying the effects of the intensity of magnetic field on the flow and temperature field, the effect of variations of other various parameters such as Rayleigh number, the angle of position of enclosure with respect to horizon, the angle of magnetic field exertion and enclosure aspect ratio on flow and temperature field is examined.

The present study deals with the natural convection in a tilted cavity filled with an electrically conducting fluid with partially thermally active vertical walls, for three different aspect ratios and three different combinations of active locations in the presence of external magnetic field perpendicular to active walls. The active part of the right side wall is at a higher temperature than the active part of the left side. The results are displayed graphically in the form of stream function and isotherms, which show the effect of magnetic field with different heating locations of the side walls, different Rayleigh numbers, different aspect ratios and different inclination angles.

2. PROBLEM DEFINITION AND MATHEMATICAL MODEL

The geometry and the coordinate system are schematically shown in Figure 1. Magnetic field of strength B_0 is applied parallel to the x-axis. The partially thermally active side walls of the cavity are maintained at two different but uniform temperatures, namely T_h and T_c, respectively, with $T_h > T_c$, and the bottom wall, the top wall and remaining parts of the side walls are insulated. Three Different cases are studied when the hot and cold location is moving over side wall. These cases are middle-middle, bottom-top and top-bottom location.

In Figure 1, L and H denote width and height of the cavity, respectively and ϕ is the tilted angle with respect to horizon. The ratio of H/L is aspect ratio and denoted as AR.

The mass, linear momentum and energy equations are as follow, respectively:

$$\frac{\partial u}{\partial x}+\frac{\partial v}{\partial y}=0 \tag{1}$$

$$\rho\left(u\frac{\partial u}{\partial x}+v\frac{\partial u}{\partial y}\right)= -\frac{\partial p}{\partial x}+\mu\left(\frac{\partial^2 u}{\partial x^2}+\frac{\partial^2 u}{\partial y^2}\right)+\rho g\beta\sin\phi(T-T_c) \tag{2}$$

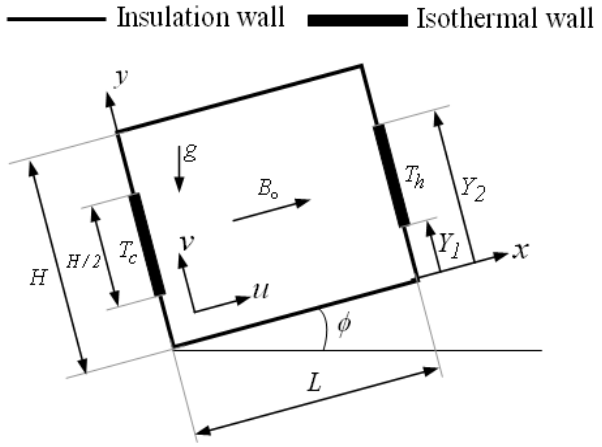

Figure 1. Geometry and coordinates of cavity configuration.

$$\rho\left(u\frac{\partial v}{\partial x}+v\frac{\partial v}{\partial y}\right)= -\frac{\partial p}{\partial y}+\mu\left(\frac{\partial^2 v}{\partial x^2}+\frac{\partial^2 v}{\partial y^2}\right)+\rho g\beta\cos\phi(T-T_c)-\sigma v B_0^2 \tag{3}$$

$$u\frac{\partial T}{\partial x}+v\frac{\partial T}{\partial y}=\alpha\left(\frac{\partial^2 T}{\partial x^2}+\frac{\partial^2 T}{\partial y^2}\right) \tag{4}$$

Where u and v are the velocity components, p is the pressure, T is the temperature, α is the thermal diffusivity, ρ is the density, g is the gravitational acceleration, μ is the viscosity, β is the coefficient of thermal expansion, B_0 is the magnitude of magnetic field and σ is the electrical conductivity.

With defining the below dimensionless variables:

$$X=\frac{x}{L},\quad Y=\frac{y}{L},\quad U=\frac{uL}{\alpha},\quad V=\frac{vL}{\alpha},\quad P=\frac{pL^2}{\rho\alpha^2},\quad \theta=\frac{T-T_c}{T_h-T_c}$$

The governing equations in dimensionless form become as:

$$\frac{\partial U}{\partial X}+\frac{\partial V}{\partial Y}=0 \tag{5}$$

$$U\frac{\partial U}{\partial X}+V\frac{\partial U}{\partial Y}=-\frac{\partial P}{\partial X}+Pr\left(\frac{\partial^2 U}{\partial X^2}+\frac{\partial^2 U}{\partial Y^2}\right)+Ra\,Pr\,\theta\sin\phi \tag{6}$$

$$U\frac{\partial V}{\partial X}+V\frac{\partial V}{\partial Y}= -\frac{\partial P}{\partial Y}+Pr\left(\frac{\partial^2 V}{\partial X^2}+\frac{\partial^2 V}{\partial Y^2}\right)+Ra\,Pr\,\theta\cos\phi-VHa^2\,Pr \tag{7}$$

$$U\frac{\partial\theta}{\partial X}+V\frac{\partial\theta}{\partial Y}=\left(\frac{\partial^2\theta}{\partial X^2}+\frac{\partial^2\theta}{\partial Y^2}\right) \tag{8}$$

where Pr, Ra, and Ha are the Prandtl, Rayleigh and Hartmann numbers and are defined as follows:

$$Pr=\frac{\nu}{\alpha}\qquad Ra=\frac{g\beta(T_h-T_c)L^3}{\alpha\nu}\qquad Ha=B_0L\sqrt{\frac{\sigma}{\rho\nu}} \tag{9}$$

where ν is the dynamic viscosity. The effect of the electromagnetic field is introduced into the equations of motion through the Lorentz force term, $\vec{J}\times\vec{B}$, which is the vector product of the electric current density $\vec{J}$ and magnetic field inductance $\vec{B}$. The magnetic Reynolds number, $Re_m = UL/\lambda$, is very small (i.e. $Re_m << 1$) in most of the engineering applications so that the magnetic field, $\vec{B}$, is unchanged by the flow λ is equal to $(\mu\sigma)^{-1}$.

The electric current density $\vec{J}$ is calculated from Ohm's phenomenological law as:

$$\vec{J} = \sigma(-\vec{\nabla}\Phi + \vec{V}\times\vec{B}) \quad (10)$$

Where, $\vec{V}$ is the velocity vector and Φ is the electric potential.

The conservation of the electric charge is:

$$\vec{\nabla}.\vec{J} = 0 \quad (11)$$

From Equations 10 and 11 a Poisson equation for Φ is easily derived:

$$\nabla^2\Phi = \vec{\nabla}.(\vec{V}\times\vec{B}) \quad (12)$$

Velocity vector and magnetic field are equal to:

$$\vec{V} = u\hat{e}_x + v\hat{e}_y$$

$$\vec{B} = B_0\hat{e}_x \quad (13)$$

From Equations 12 and 13, Poisson equation for Φ is equal to:

$$\nabla^2\Phi = -B_0\partial v/\partial z \quad (14)$$

In two-dimensional frame, $\partial v/\partial z$ equal zero and hence:

$$\nabla^2\Phi = 0 \quad (15)$$

Since always there is somewhere around the cavity an electrically insulating boundary on which $\partial\Phi/\partial n = 0$, the unique solution for Equation 15 is $\vec{\nabla}\Phi = 0$, which means that the electric field vanishes everywhere. The Lorentz force then reduces to a systematically damping factor $-\sigma B_0{}^2 v$.

The boundary conditions are:

at all walls (X=0,X=1,Y=0,Y=H/L) $U \& V = 0$

at right active part $\theta = 1$

at left active part $\theta = 0$

at adiabatic walls $\partial\theta/\partial n = 0$

In order to compare total heat transfer rate, Nusselt number is used. The average Nusselt numbers are defined as follows:

$$\overline{Nu} = 2\int_{Y_1}^{Y_2} \left.\frac{\partial\theta}{\partial X}\right|_{X=1} dY \quad (16)$$

Where Y_1 and Y_2 are dimensionless lengths shown in Figure 1.

The stream function used for comparing the flow characteristics is determined by the following equation:

$$\frac{\partial\psi}{\partial Y} = -U \quad (17)$$

3. NUMERICAL PROCEDURE

The governing equations associated with the boundary conditions were solved numerically using the control-volume based finite volume method. The hybrid-scheme, which is a combination of the central difference scheme and the upwind scheme, was used to discretize the convection terms. A staggered grid system, in which the velocity components are stored midway between the scalar storage locations, was used. In order to couple the velocity field and pressure in the momentum equations, the well known SIMPLER-algorithm was adopted [10]. Grid dependency was investigated for the standard case. The solution of the fully coupled discretized equations was obtained iteratively using the TDMA method.

1.3. Choice a Suitable Grid Uniform staggered grid system is employed in the present study. To obtain a suitable grid, the vertical velocity profile

at center line of the cavity, V_c, for grid 41 × 41, 51 × 51, 61 × 61, 71 × 71 and 81 × 81 at Ra = 10^5 and Ha = 10 for middle-middle active location are shown in Figure 2. As shown, grid 61 × 61 is sufficiently fine to ensure a grid independent solution.

2.3. Code Validation In order to make sure that the developed codes are free of error coding, a validation test was conducted. The present results are compared with those of Rudraiah, et al [5] in Table 1.

Data from the table shows that the results of the present work, even though there are some differences, do agree very well with the previous work results.

Based on this successful validation, the problem is solved by using the code.

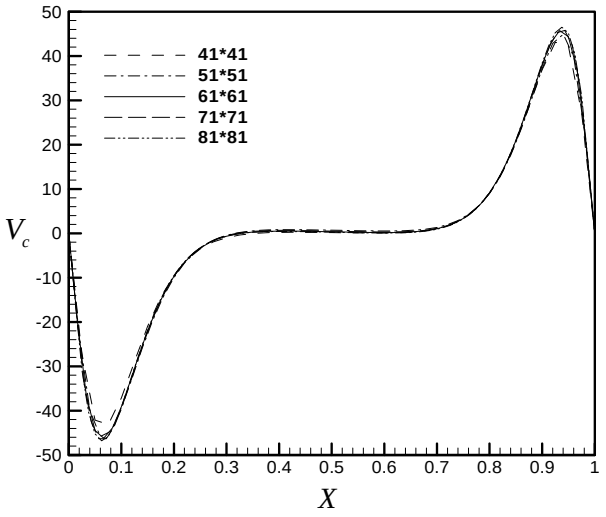

Figure 2. Vertical velocity profile for different grid for middle-middle active location, $Ra=10^5$ and $Ha=10$.

4. RESULT AND DISCUSSION

Numerical computations in the present study were carried out for Pr = 0.71. The effect of magnetic field on the buoyancy-driven convection of an electrically conducting fluid in a tilted cavity, with partially thermally active side walls is investigated numerically. The inclination angle of the cavity was chosen to be 0˚, 30˚, 60˚ and 90˚. AR was selected as 0.5 (shallow cavity), 1.0 (square cavity) and 2.0 (tall cavity). The buoyancy force is naturally more effective for higher Rayleigh numbers. The Lorentz force reduces velocities and suppresses the convection. The both forces are equally effective when $Ra/Ha^2 = O(1)$. The buoyancy is dominant as long as $O(Ra/Ha^2) << 1$ and the magnetic field is dominant when $O(Ra/Ha^2) >> 1$. The Hartmann number was taken in the range 0–100. The Rayleigh number was varied in the range 10^4-10^6 to cover both buoyancy and magnetic field dominant flow regimes. The flow fields and the temperature gradients inside the tilted cavity are presented to illustrate the impact of the magnetic field and positioning of the active locations on the heat transfer characteristics. The heated location is kept on the right wall and the cooled location on the left wall.

TABLE 1. Comparison of the Present Results with the Rudraiah Results [5].

Gr	Ha	$\overline{Nu}$	
		Rudraiah, et al [5]	Present Work
2×10^4	0	2.5188	2.503
	10	2.2234	2.213
	50	1.0856	1.083
	100	1.0110	1.009
2×10^5	0	4.9198	4.949
	10	4.8053	4.761
	50	2.8442	2.633
	100	1.4317	1.447
2×10^6	0	8.7030	9.310
	10	8.6463	9.200
	50	7.5825	7.125
	100	5.5415	4.633

4.1. Effect of Active Locations on Flow Field and Heat Transfer Figures 3 and 4 show the streamlines and isotherms for three different combinations of active locations and three different Rayleigh number for Ha = 10. In Figure 3 the buoyancy force moves the fluid particles heated near the hot wall toward the cold location. We can see that axis of vortices moves as the locations of active parts are changed. In the case of Ra = 10^5

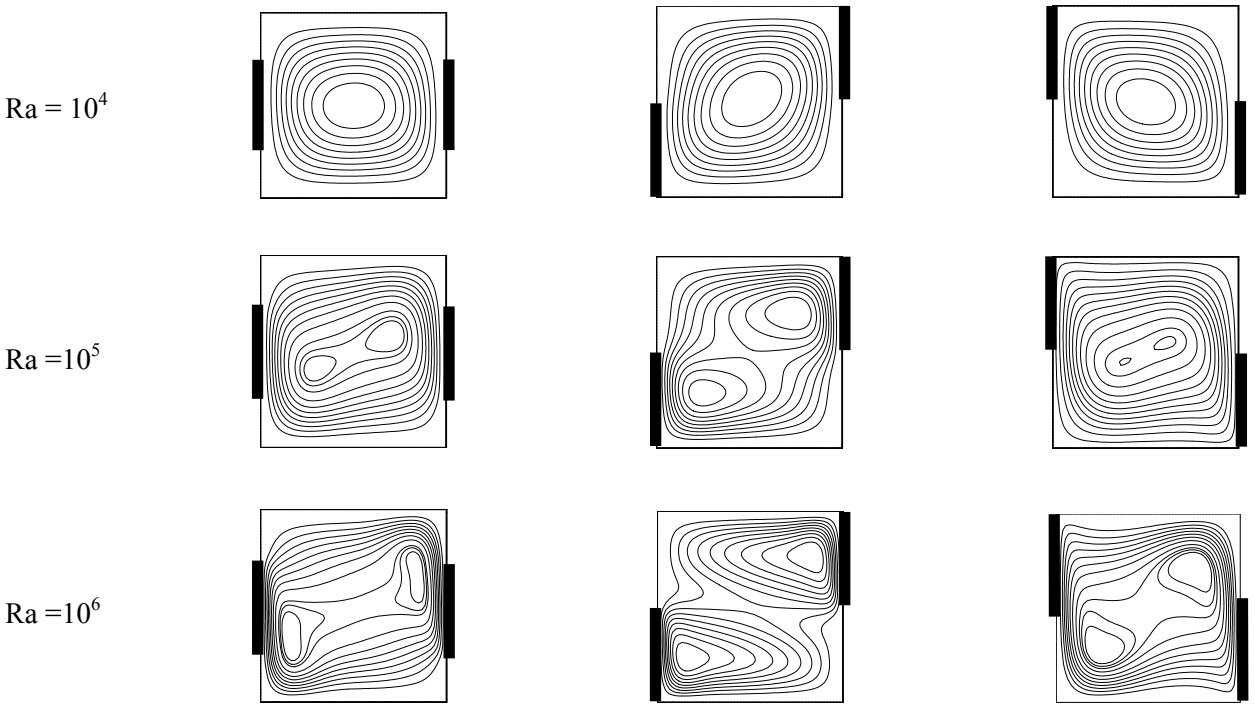

Figure 3. Stream function plots for different locations and different Ra at Ha = 10.

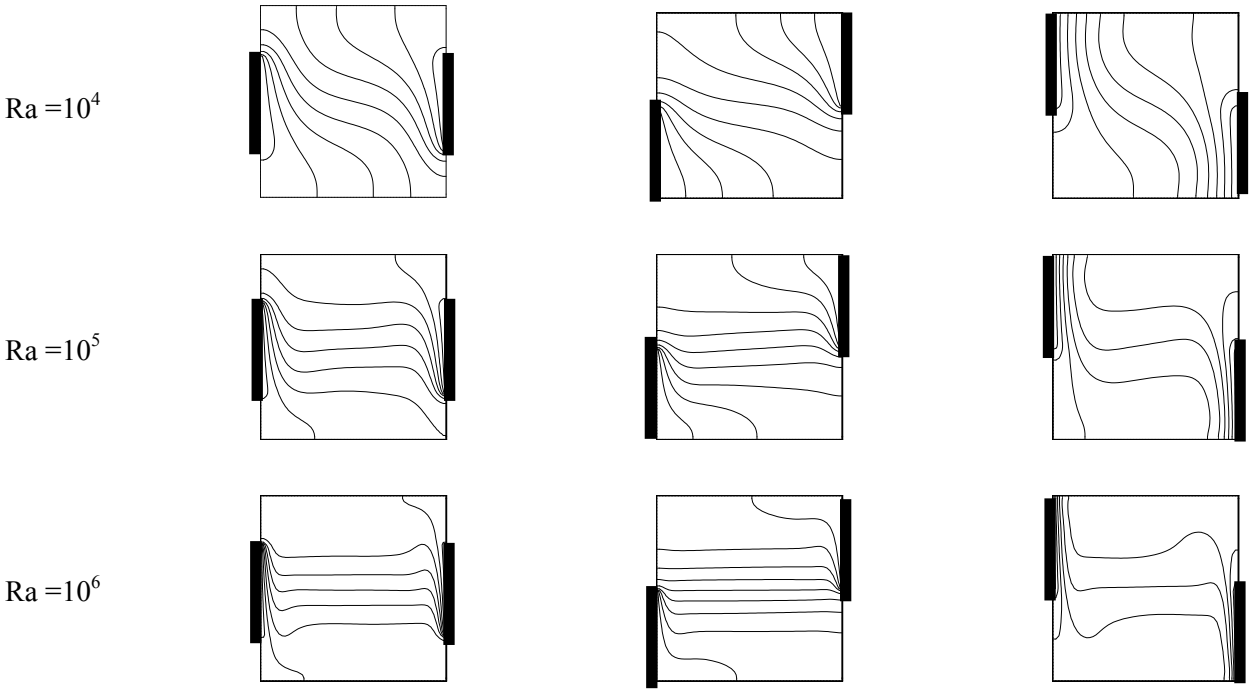

Figure 4. Isotherms plots for different locations and different Ra at Ha = 10.

and Ra = 10^6, two fully developed counter clockwise rotating vortices are seen inside the cavity, that with increase Ra, they become farther from each other. In the case of bottom-top active locations the streamlines are denser near the active parts.

For all values of Ra, the maximum absolute value of the stream function ($|\psi|_{max}$) for the case of bottom-top location is smaller than the case of middle-middle and top-bottom, respectively. For example, for Ra = 10^5 and Ha = 10, for bottom-top location case, $|\psi|_{max}$ = 3.136, and for the middle-middle and top-bottom cases $|\psi|_{max}$ = 6.395 and $|\psi|_{max}$ = 9.491. From Figure 4, it is observed that, with increasing Ra, convection strength increases. In the all cases of Ra = 10^4 and Ra = 10^5 have been shown that the corresponding isotherms are almost parallel to the horizontal wall at the center of the cavity as the flow is stagnant at the core and convection mode of heat transfer prevails all over the cavity except at the center that dominant of heat convection is conduction.

As shown in Figure 5, for the case of middle-middle Nusselt number is more than top-bottom and bottom-top cases, respectively.

4.2. Effect of Active Locations and Aspect Ratio on Flow Field and Heat Transfer Figures 6 and 7 show the streamlines and isotherms for three different combinations of active locations, three different AR, Ra =10^5 and Ha = 10. In the case AR = 2 only in the bottom-top location two fully developed counter clockwise rotating vortices are seen in the core of cavity, but in the case AR = 1 in all active locations two fully developed counter clockwise rotating vortices are seen. For AR = 0.5 in the core of cavity, there is a single fully developed counter clockwise rotating vortex. In all AR, it is observed that the maximum absolute value of the stream function for top-bottom is more than middle-middle and bottom-top, respectively. The maximum absolute value of the stream function for AR = 0.5 is more than AR = 1 and 2 respectively in all active locations. For example, in Ha = 10 and Ra = 10^5 for case of top-bottom active location and AR = 0.5, 1, 2 the maximum absolute value of the stream function is 9.5, 9.4, 9.03 respectively.

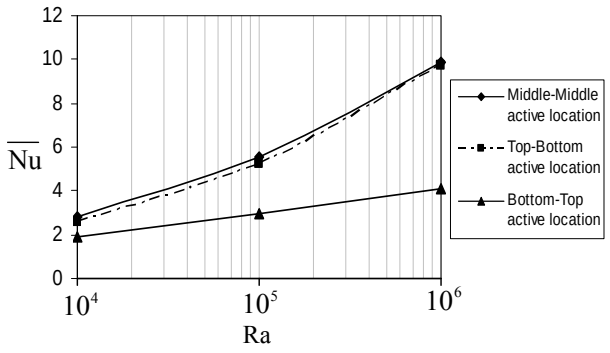

Figure 5. Effect of Ra on average nusselt number for different locations at Ha = 10.

As shown in Figure 7, for AR = 1 the isotherms are almost parallel to the horizontal wall at the center of the cavity and the fluid is stagnant at the core and convection mode of heat transfer prevails all over the enclosure except at the center. In AR = 2 this case is observed only at bottom-top active location case. The Nusselt number increases with increasing AR as shown in Figure 8, especially in middle-middle active location.

4.3. Effect of Hartmann Number on Flow Field and Heat Transfer Figures 9 and 10 show the stream function and isotherms for the case of middle-middle active location for various Ha and Ra at cavity with AR = 1. According to Figure 9, at Ra = 10^4, a single vortex parallel with horizontal wall at the core of cavity is seen, which with increasing Ha become vertical. At Ra = 10^5 and 10^6 it is observed that two fully developed counter-clockwise rotating vortices inside a large cell are formed, that with increasing Ha are change into single vortex. It is to be noted that in Ra = 10^6 this change is occurred at higher Ha.

At Ra = 10^4, it is observed that the heat transfer between the hot and cold walls is carried out by conduction and convection but by applying a magnetic field (Ha=100) we can suppress the natural convection so that the maximum absolute value of the stream function reaches to $|\psi|_{max}$ = 0.11, which at Ha = 0 it was $|\psi|_{max}$ = 4.12. It means that the movement of fluid is very small or in other words the fluid is stagnant. In this case heat transfer between right and left walls occurs only by conduction and the isotherms will be vertical.

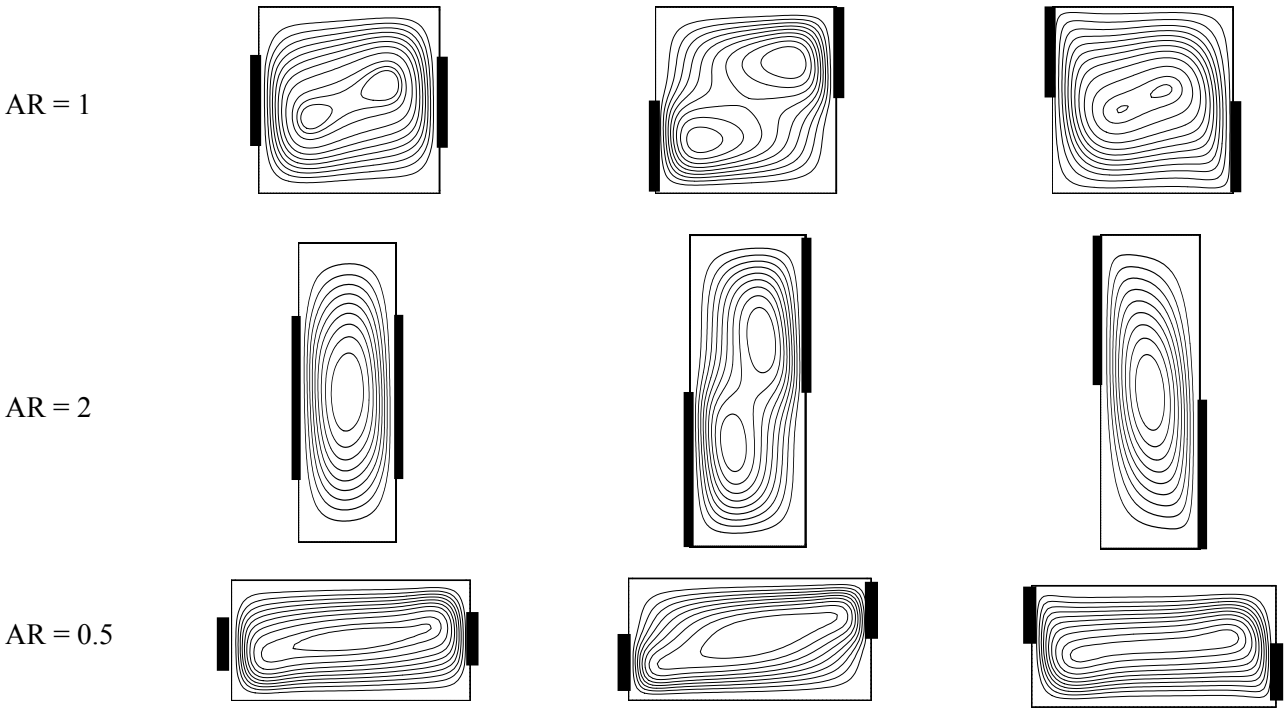

Figure 6. Stream function plots for various locations and various AR at Ra =10^5 and Ha = 10.

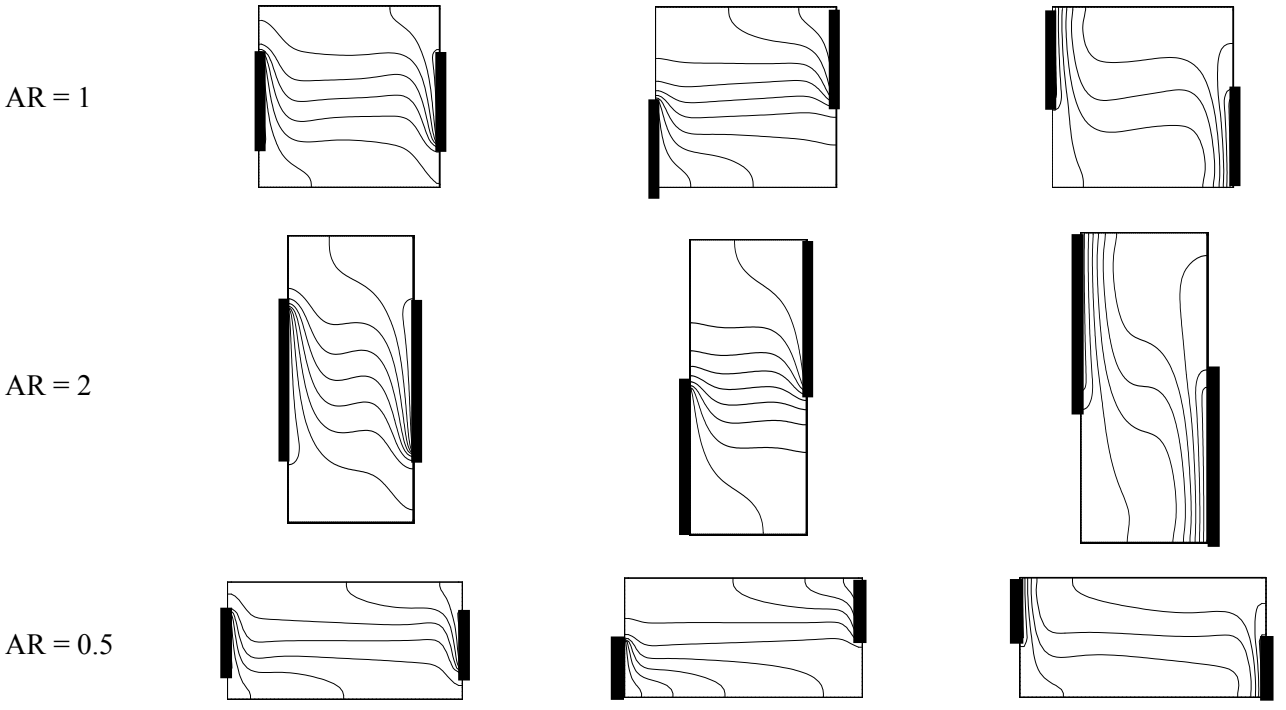

Figure 7. Isotherms plots for various locations and various AR at Ra =10^5 and Ha = 10.

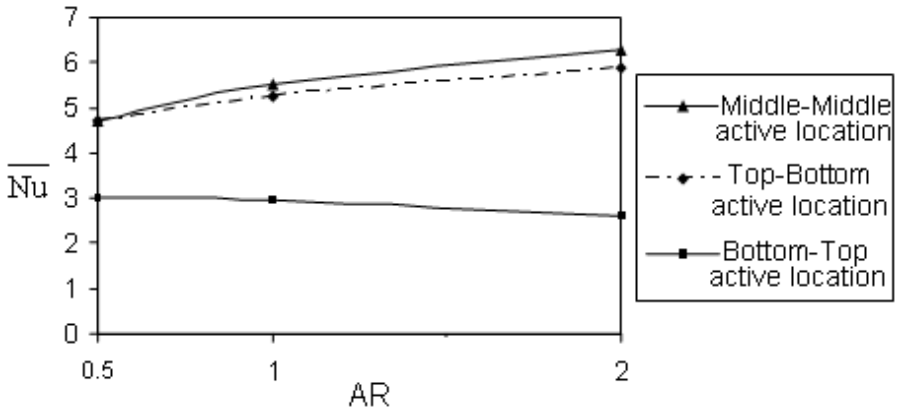

Figure 8. Effect of Ar on average nusselt number for different locations, Ra = 10^5 and Ha = 10.

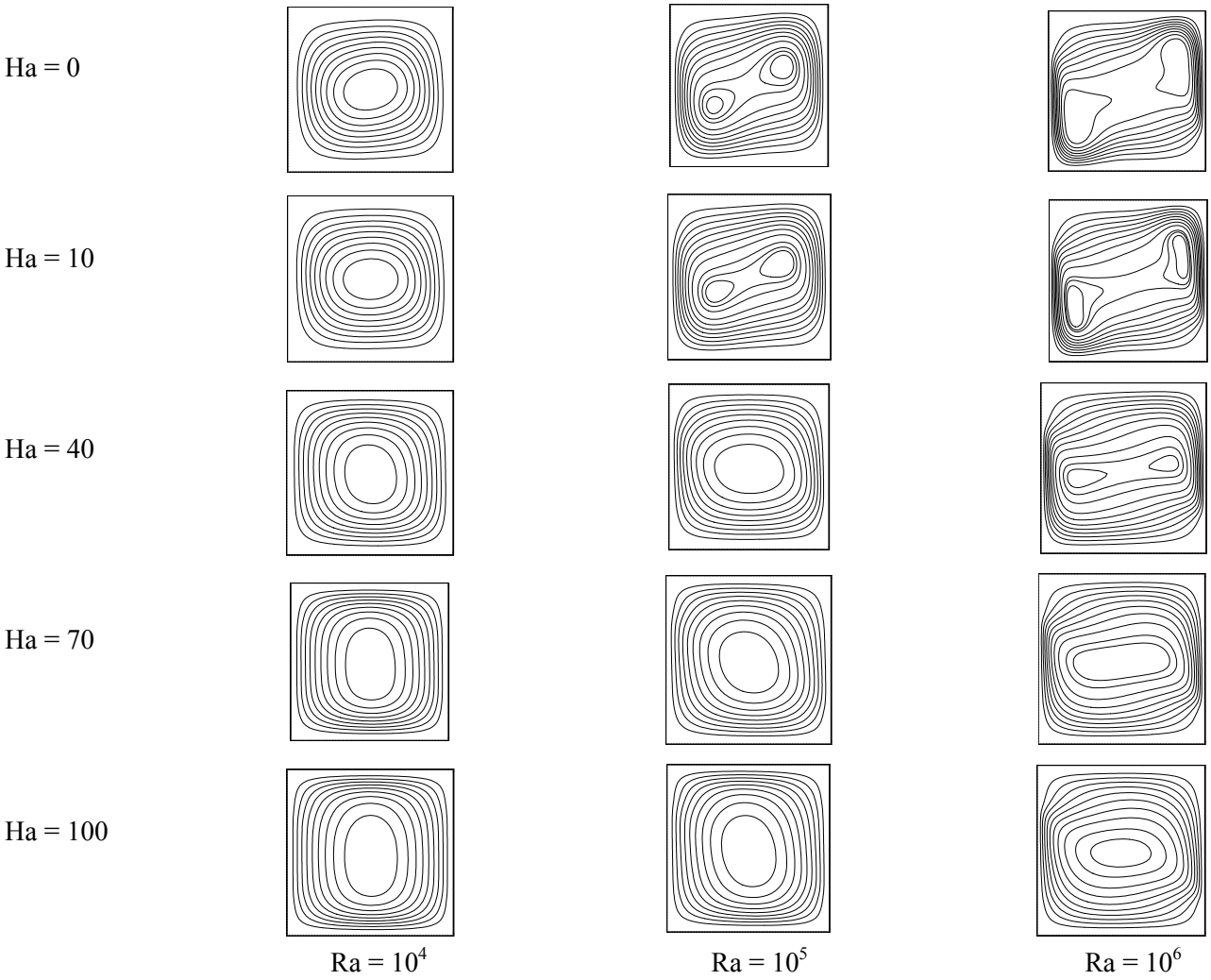

Figure 9. Stream function plots for various Ha and Ra for middle-middle active location.

At Ra = 10^5, the convection becomes more important ($|\psi|_{max}$=7.09) and isotherms are more distorted. At Ha = 100, it is found that convection significantly decreases ($|\psi|_{max}$=1.03) and the isotherms become modified. As Ra increases to 10^6, the heat transfer mechanism changes into a relatively pure convection and the influence of the magnetic field is weaker.

The temperature profiles at high Ha (Ha=100) indicate that the heat transfer process is still controlled by both conduction and convection mechanisms.

The effects of the magnetic field on the average Nusselt number at various Rayleigh numbers is shown in Figure 11. It is evident from this figure that for the all values of Ra, by increasing Ha, the Nu approaches unity; indicating a pure conduction regime. Furthermore, it is observed that as the value of Ra is increased, the convective heat transfer is increased, so that for suppression of convection very high strength magnetic field is needed. The variation of vertical velocity in center line of cavity with Ha is shown in Figure 12. We see that with increasing Ha, vertical velocity decrease.

Variation of average Nusselt number in terms of Ha for various AR is shown in Figure 13. From this figure we see that at AR = 0.5 heat transfer is lower than AR = 1 and AR = 2.

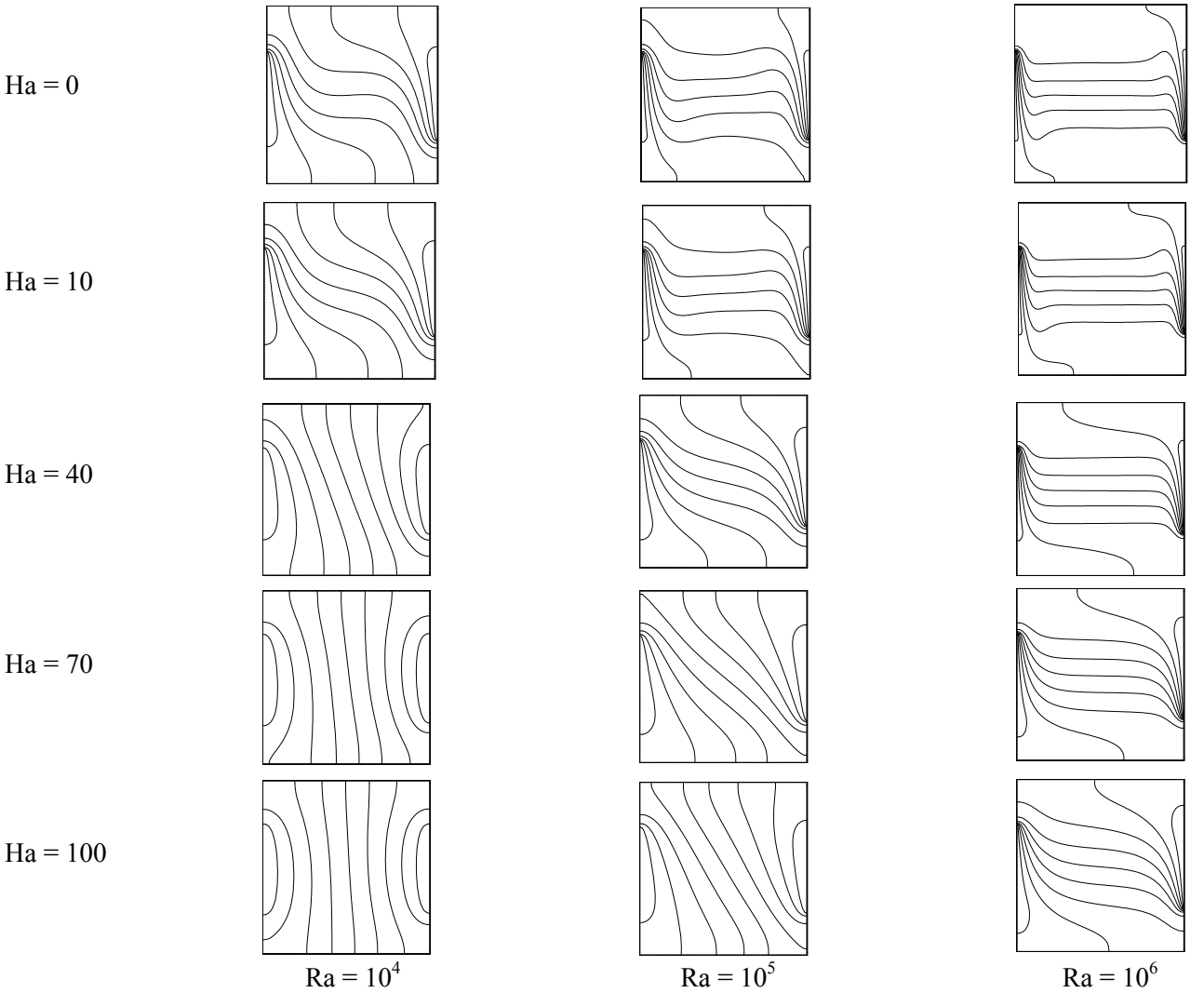

Figure 10. Isotherm plots for various Ha and Ra for middle-middle active location.

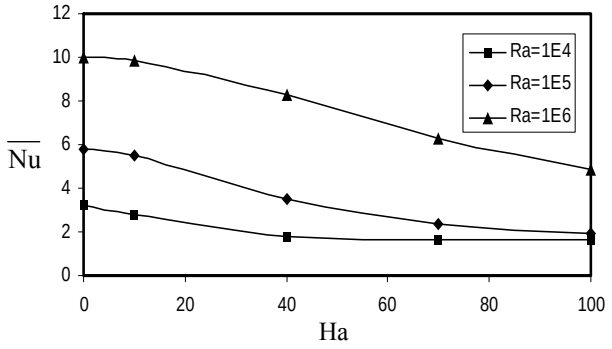

Figure 11. Effect of Ha on average Nusselt number for middle-middle location and various Ra.

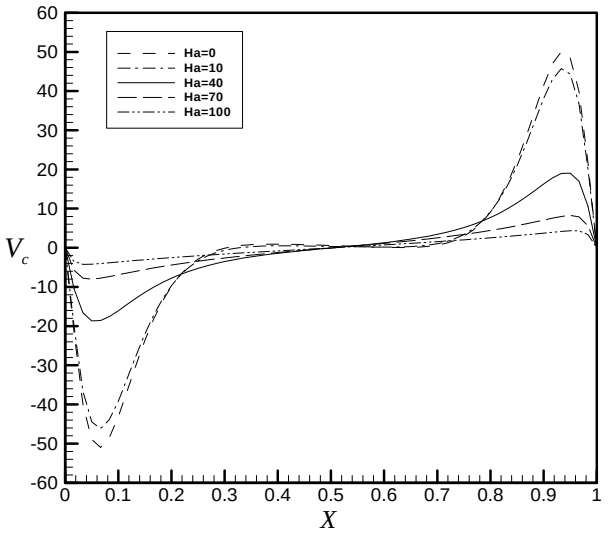

Figure 12. Variation of vertical velocity in center line of enclosure with change in Ha for Ra = 10^5 and middle-middle active location.

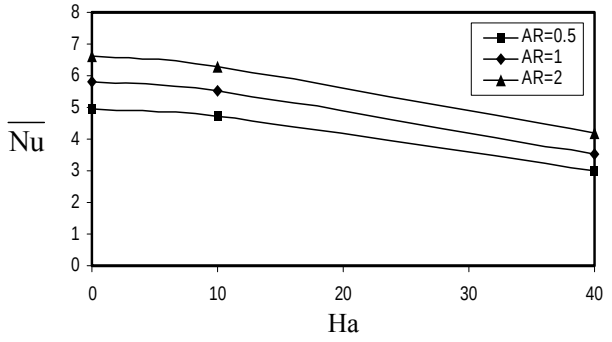

Figure 13. Effect of Ha on average Nusselt number for middle-middle location, different AR and Ra = 10^5.

4.4. Effect of Inclination Angle on Flow Field and Heat Transfer Figures 14 and 15 show the stream function and isotherms for case of middle-middle active location for various Ha and various inclination angle at Ra = 10^5 for a cavity with AR = 1.

As we can see from Figure 14, at lower Ha and in inclination angle between 0˚ and 60˚ ($0^\circ<\phi<60^\circ$) with increasing ϕ, two vortex in the center of cavity are suppressed and change into single vortex. Also from Figure 14 we can see in $\phi = 90^\circ$ and Ha = 100, two small vortex and two big vortex is formed in enclosure. It is evident from Figure 15 that the intensity of the core convection is considerably decreased due to the drag force induced by the magnetic field; as indicated by a weak distortion of the isothermal lines.

This effect is more pronounced at smaller inclination angles ($0^\circ<\phi<60^\circ$) and diminishes considerably for higher inclination angle ($\phi=90^\circ$).

Figure 16 shows the variation of Nusselt number in terms of inclination angle for Ra = 10^5 and different Ha. We see that from $\phi = 0^\circ$ to $\phi = 30^\circ$ average Nusselt number increase and from $\phi = 30^\circ$ to $\phi = 90^\circ$ Nusselt number decreases. Also Table 2 shows the average Nusselt number for various Ra, Ha and ϕ.

5. CONCLUSIONS

In this paper, the effect of an imposed magnetic field on flow field and heat transfer in a tilted cavity with partially active locations was studied numerically. From this study it was found that heat transfer can be decreased by these methods: choosing the bottom-top as the active location, *AR*=0.5, increasing the Hartmann number, and increasing the inclination angle in the range of 30˚ and 90.

6. NOMENCLATURE

AR	Aspect ratio
B_0	Magnetic field strength

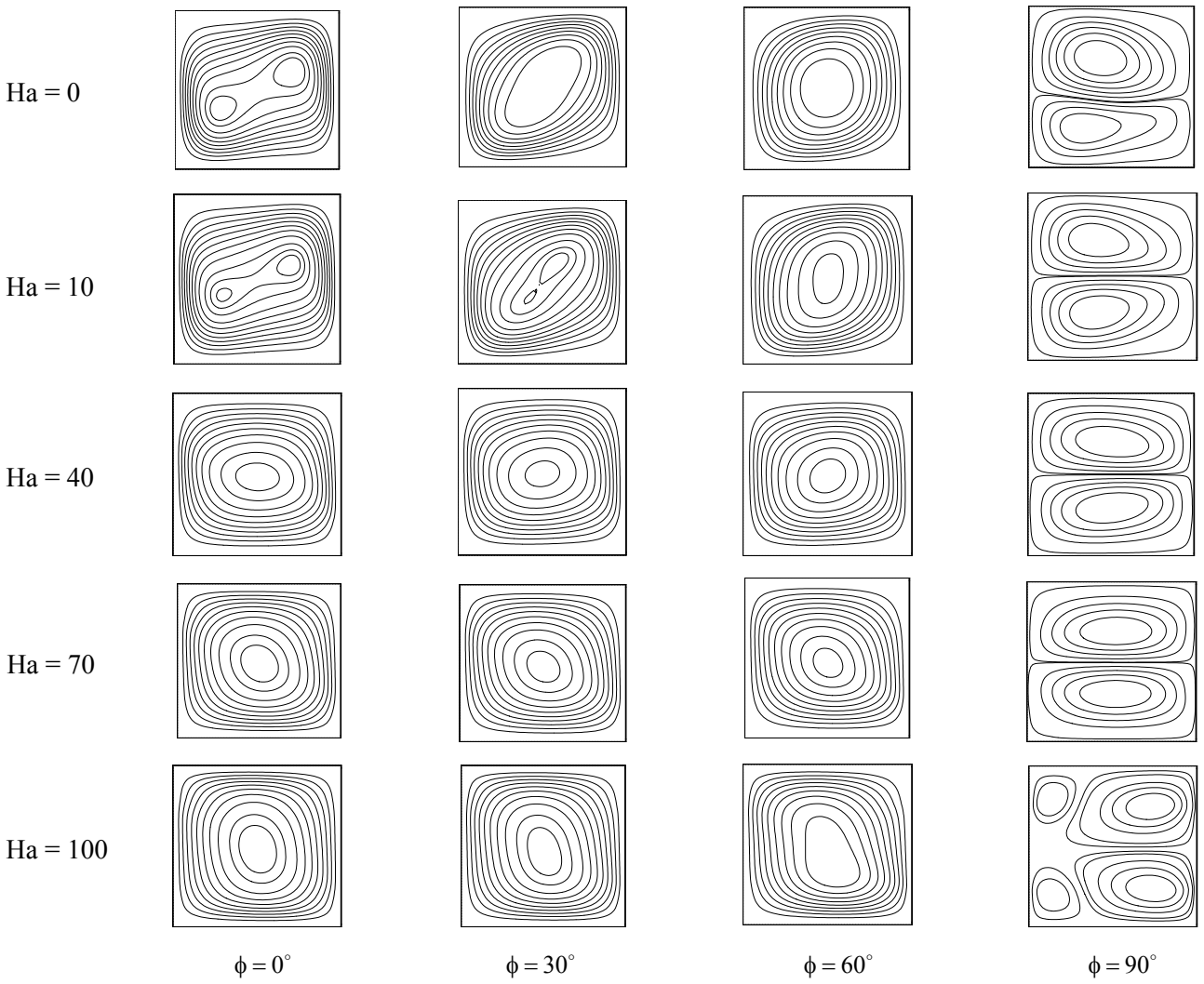

Figure 14. Stream function plots for different inclination angle and Ha for Ra = 10^5 and middle-middle location.

Ha	Hartmann number
J	Current density
$\overline{Nu}$	Average Nusselt number
Pr	Prandtl number
Ra	Rayleigh number
Re_m	Magnetic Reynolds number
u, v	Velocity components
U,V	Dimensionless velocity components

Greek Letters

α	Thermal diffusivity
β	Coefficient of thermal expansion
ν	Kinematic viscosity
θ	Dimensionless temperature
σ	Electrical conductivity of the medium
Φ	Electric potential
ϕ	Angle of inclination of the enclosure
ψ	Stream function

7. REFERENCES

1. Davidson, P.A., "An Introduction to Magneto hydrodynamic", Cambridge University Press, Cambridge, U.K., (2001), 3-24.

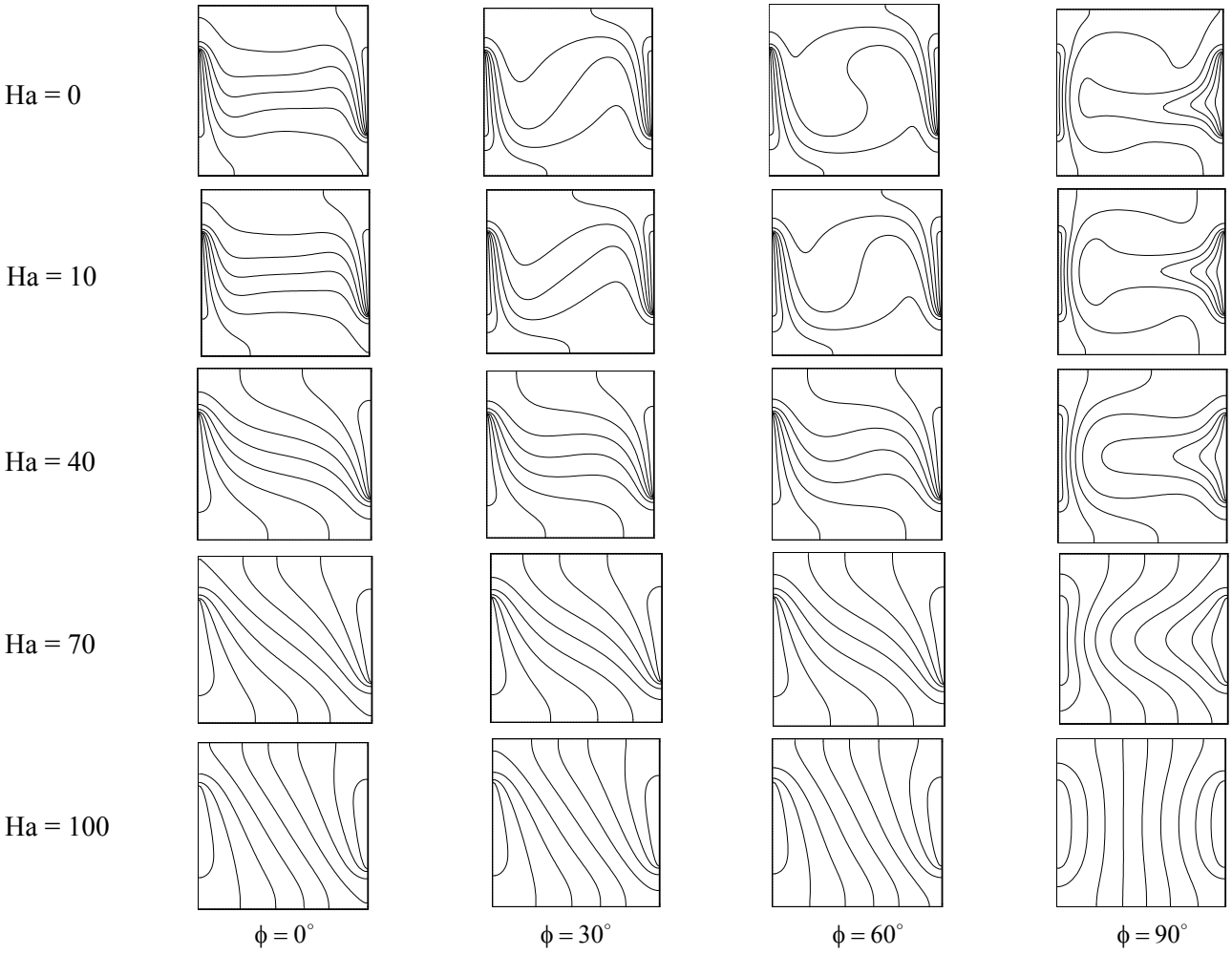

Figure 15. Isotherm plots for different inclination angle and Ha for Ra = 10^5 and middle-middle location.

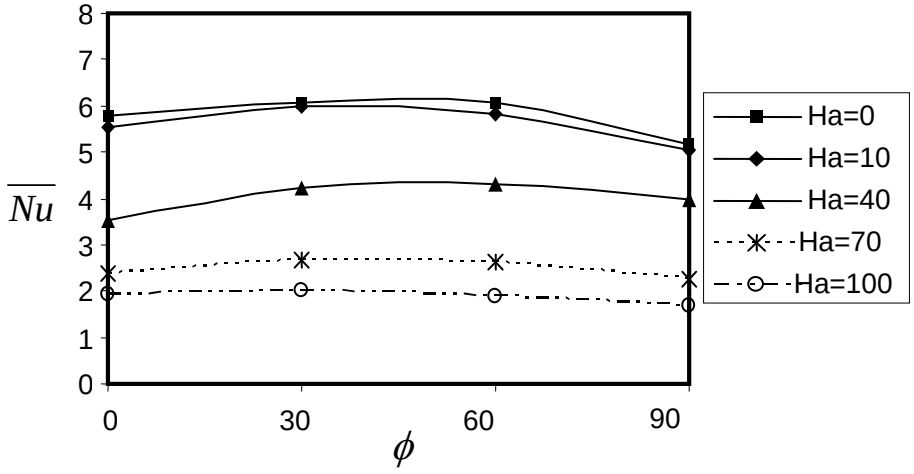

Figure 16. Variation of Nusselt number for different inclination angle and Ha for Ra=10^5 and middle-middle location.

TABLE 2. Average Nusselt number for Various Ra, Ha and ϕ.

Ra	Ha	$\overline{Nu}$			
		$\phi = 0^\circ$	$\phi = 30^\circ$	$\phi = 60^\circ$	$\phi = 90^\circ$
10^4	0	3.211	3.586	3.610	3.283
	100	1.666	1.667	1.663	1.662
10^5	0	5.788	6.084	6.057	5.1611
	100	1.941	2.000	1.882	1.668
10^6	0	9.978	10.150	9.854	8.571
	100	4.860	6.000	5.953	5.872

2. Oreper, G.M. and Szekely, J., "The Effect of an Externally Imposed Magnetic Field on Buoyancy Driven Flow in a Rectangular Cavity", ***Journal of Crystal Growth***, Vol. 64, No. 3, (1983), 505-515.
3. Ozoe, H. and Maruo, M., "Magnetic and Gravitational Natural Convection of Melted Silicon-Two Dimensional Numerical Computations for the Rate of Heat Transfer", ***JSME International Journal***, Vol. 30, No. 263, (1987), 774-784.
4. Garandet, J.P., Alboussiere, T. and Moreau, R., "Buoyancy Driven Convection in a Rectangular Enclosure With a Transverse Magnetic Field", ***International Journal of Heat and Mass Transfer***, Vol. 35, No. 4, (1992), 741-748.
5. Rudraiah, N., Barron, R.M., Venkatachalappa, M. and Subbaraya, C.K., "Effect of a Magnetic Field on Free Convection in a Rectangular Enclosure", ***International Journal of Engineering Science***, Vol. 33, No. 8, (1995), 1075-1084.
6. Alchaar, S., Vasseur, P. and Bilgen, E., "The Effect of a Magnetic Field on Natural Convection in a Shallow Cavity Heated From Below", ***Chemical Engineering Communications***, Vol. 134, No. 1, (1995), 195-209.
7. Al-Najem, N.M., Khanafer, K.M. and El-Refaee, M.M., "Numerical Study of Laminar Natural Convection in Tilted Enclosure with Transverse Magnetic Field", ***International Journal of Numerical Methods for Heat and Fluid Flow***, Vol. 8, No. 6, (1998), 651672.
8. Kandaswamy, P., Malliga Sundari, S. and Nithyadevi, N., "Magnetoconvection in an enclosure with partially active vertical walls", ***International Journal of Heat and Mass Transfer***, Vol. 51, No. 7-8, (2008), 1946-1954.
9. Babaei, M.R., "Parametric Study of Effect an Imposed Magnetic Field on Natural Convection and Heat Transfer in a Two Dimensional Cavity", MS.c thesis, Department of Mechanical Engineering, University of Kashan, Kashan, Iran, (2008).
10. Patankar, S.V., "Numerical Heat Transfer and Fluid Flow", McGraw-Hill, Washington, DC, U.S.A., (1980).